NATIONAL ADVISORY COMMITTEE FOR AERONAUTICS

TECHNICAL NOTE 3260

SMOKE STUDY OF NOZZLE SECONDARY FLOWS IN A LOW-SPEED TURBINE

By Milton G. Kofskey and Hubert W. Allen

Lewis Flight Propulsion Laboratory
Cleveland, Ohio

Washington
November 1954

NATIONAL ADVISORY COMMITTEE FOR AERONAUTICS

TECHNICAL NOTE 3260

SMOKE STUDY OF NOZZLE SECONDARY FLOWS IN A LOW-SPEED TURBINE

By Milton G. Kofskey and Hubert W. Allen

SUMMARY

Smoke was used to visualize boundary-layer and wake secondary-flow phenomena in the nozzle passages of a low-speed turbine, and the flow patterns were recorded in both still and motion pictures. The two annular cascades of turbine nozzles which were used were designed for constant discharge angle from hub to tip, but they differed in blade shape and suction-surface velocity distribution. Cross-channel secondary flows were similar for both cascades, but radial-flow patterns and outer-shroud vortex formation differed. This flow behavior at low airspeed (7 ft/sec) agreed with that previously indicated for the same blades by pressure and flow-angle measurements near sonic speed.

The effect of a downstream rotor on nozzle secondary flows was also studied. Motion of the rotor blade row disturbed nozzle trailing-edge radial flows at low rotor speeds and produced pulsations in the radial flow from the outer shroud. At increased rotor speed the amplitude of the radial-flow pulsations decreased.

The motion pictures prepared as a supplement to this report may be obtained on loan from NACA Headquarters, Washington, D.C.

INTRODUCTION

When fluid in an annular cascade is turned, the resulting mainstream pressure gradients are imposed on the boundary layers of low-momentum fluid on the walls and blades. Boundary-layer turning equal to the free-stream turning is not sufficient to balance the imposed pressure gradients and the centrifugal forces associated with motion along a curved path. Therefore, more than free-stream turning of the low-momentum boundary-layer fluid results.

Experimental investigations of these deviations of flow direction in boundary layers and wakes, herein referred to as secondary flows, are reported in references 1 and 2. The object of these studies was to

clarify the nature and causes of such flows and to present information that permits an estimate of the extent of their influence on cascade and turbine performance. In reference 1, secondary flows of low-speed air in two-dimensional cascades were mapped by such visualization techniques as smoke filaments and chemical traces. In reference 2, which extended the work to turbine nozzles in annular cascades at operational airspeeds, similar patterns were obtained, with radial flows added in these three-dimensional cases. Quantitative pressure and flow-angle measurements downstream of nozzle rows indicated that cross-passage and radial flows are responsible for accumulations of low-momentum boundary-layer fluid that disturb flow-angle distributions and thereby may affect subsequent blade rows. Comparison of blades with different suction-surface contours and velocity profiles indicated that these characteristics have an important bearing on secondary-flow effects.

In order to investigate further this type of flow behavior in annular cascades of turbine nozzles, current visualization techniques were applied to a three-dimensional cascade and the secondary-flow patterns were recorded for detailed study in motion pictures. The use of very low airspeeds is necessary for smoke flow visualization in order to avoid excessive dispersion of the smoke. Interpretation of secondary-flow phenomena observed at low airspeeds depends somewhat on comparison with information gained earlier by other means at high airspeeds; and, in turn, low-speed results aid in interpreting measurements at high airspeeds. In addition, visualization provides details difficult to obtain in any other way.

In the present investigation, therefore, motion pictures of secondary-flow patterns as visualized by the use of smoke were made at low airspeeds. Two of the same annular cascades of nozzle blades that were investigated at high airspeeds (ref. 2) were used in order to compare smoke patterns with measured loss patterns. In addition, it was considered desirable to obtain an indication of the effects of a downstream rotor on nozzle secondary flow. Motion pictures were made of such effects for rotor blade speeds of the same order of magnitude as the airspeed used.

The motion pictures were prepared as a supplement to this report and may be obtained on loan from NACA Headquarters, Washington, D.C.

APPARATUS AND PROCEDURE

Test Unit

A schematic view of the test unit used in the investigation is shown in figure 1. The outer shroud was constructed of Lucite to facilitate visual inspection and photography of the smoke flow pattern through the turbine. The rotor assembly was mounted on rails to

provide quick removal of the rotor for isolated nozzle investigations. The speed of the rotor, which consisted of 29 circular-arc sheet metal blades with about 98° turning, was controlled by a variable-speed electric motor. Air to the cascade was supplied by the laboratory combustion air system and was discharged directly into the room.

The smoke traces were photographed by a still camera and two types of 16-millimeter movie camera. A nominal film speed of 32 frames per second was obtained with a standard motion-picture camera, and nominal film speeds of 300 to 1000 frames per second were obtained with a high-speed motion-picture camera. The high-speed camera contained an internal time marker that recorded time marks on the film every 1/120 second. Approximate values of film speeds, wheel speeds, and smoke speeds could be calculated from these time marks.

3269

CE-1 back

Nozzle Blades

The two configurations investigated are designated blades A and B. Blade A, which was designed by the stream-filament method, has a constant discharge angle of 56° from axial and has a smooth suction-surface velocity profile. As the stream-filament method applies only to the portion of the blades forming the channel, the blades were designed to do the greater part of the turning within the channel. The trailing-edge portions of the blades having very little curvature were faired at the approximate discharge angle. Blade B is a commercial blade designed for a constant discharge angle of approximately 60° from axial. The blade has a more blunt leading edge than blade A, the turning being accomplished over the entire blade surface from leading to trailing edge.

Suction-surface velocity profiles determined by the stream-filament method are presented in figure 2 for both blade configurations. The method of differences used in determining curvature tends to reduce the velocity gradients, so that the amplitude of the actual velocity variations is undoubtedly greater than that shown by figure 2. Mean-section blade shapes for both configurations are shown in figure 2(b).

Flow-Visualization Method

Smoke was produced by burning oil-soaked cigars in a forced draft of air. This method, which is fully described in reference 1, is superior to other methods that have been used, because the smoke is nontoxic, noncorrosive, and easily generated. The rate of smoke production and injection into the air stream was carefully controlled by means of settling bottles, pressure regulators, and bleeds so as to match closely the local direction, velocity, and density of the air streams. In order

to minimize dispersion of the smoke and maintain smoke traces intense enough for high-speed photography, the nozzle axial air velocity was kept low, at approximately 7 feet per second.

RESULTS AND DISCUSSION

Secondary Flows in Isolated Nozzle Cascades

Blade B pattern. - Cross-channel and radial flows of low-momentum air for blade B are shown in figure 3. Smoke was introduced along the outer shroud near the pressure side of the blade and at the inlet to the nozzle cascade. The circumferential pressure difference between pressure and suction surfaces resulting from turning in the blade channel caused low-momentum boundary-layer air to move across the channel from pressure to suction surface. Upon reaching the suction surface, the low-momentum air divided, some being rolled up in a vortex-like motion and swept downstream. The remainder turned sharply inward along the suction surface at the trailing edge and contributed to the region of low-momentum fluid along the junction of the suction surface and the hub.

Figure 4 indicates that, when smoke introduction was suddenly stopped, the smoke in the mainstream dissipated quickly, while smoke on the suction surface and in the outer shroud and hub loss regions was visible for a longer time. In spite of the apparent high density of smoke, the relatively great length of time required for complete dissipation of smoke in the radial-flow region, particularly in the outer-shroud and hub cores, indicates nearly stagnant regions.

Blade A pattern. - The secondary-flow phenomena for blade A were in some respects different from those just described. Figure 5 shows cross-channel flow in the outer-shroud boundary layer from pressure toward suction surface, which was of the same type as that for blade B. As the low-momentum air approached the trailing edge, however, no large outer-shroud accumulation was observed as was shown for blade B where the vortex formed. The smoke indicated a more rapid radial-flow component, which in this case was located largely in the blade wake adjacent to the trailing edge instead of in the suction-surface boundary layer. The rapid through-flow component along the suction surface swept a greater part of the low-momentum air into the wake from the blade trailing edge than entered the wake for blade B, while the rest of the low-momentum air flowed radially into the vortex-like core at the hub.

When the smoke source was shut off, the smoke in the radial-flow region along the trailing edge dissipated quickly, but that in the core region near the hub remained visible for a relatively long time.

Effect of blade characteristics. - The blunt leading edge, irregular suction-surface velocity distribution, and suction-surface curvature near

the trailing edge of blade B might be expected to cause a thick or possibly separated suction-surface boundary layer that would provide a path for radial flow. Hence, there seems to be a definite connection between these blade shape features and the secondary-flow differences between blades A and B. One of these differences, which are shown in the still and motion pictures, is an outer-shroud passage vortex that appears for blade B but not for blade A. Another is a suction-surface radial flow to the hub, which is much more pronounced for blade B. A third is the more rapid downstream flow on the suction surface for blade A, which sweeps low-momentum air into the wake, whereas blade B has a less pronounced wake.

Measurements of total pressure and resulting kinetic-energy loss immediately downstream of these nozzles are reported in reference 2. In order to compare the low-speed smoke patterns reported here with the loss patterns obtained in high-speed air for reference 2, the loss patterns for the two blade configurations are shown in figure 6. These loss patterns are shown in a circumferential-radial plane as seen looking downstream into the nozzle discharge. As was also indicated by the smoke pictures, blade B has high loss regions near inner and outer shrouds with corresponding small magnitude of loss in the wake. Blade A shows no similar outer-shroud loss region but indicates a slightly higher loss region near the inner shroud, with a greater percentage of the low-momentum air swept off into the wake.

Wake phenomena. - Figure 7, obtained from the low-speed tests, shows that the wake has the tendency to form a columnar pattern. The air appears to be rolling off the blade surfaces in a series of vortices whose axes are parallel to the blade trailing edge. This effect was observed for both blade types.

Vortex patterns. - Figures 8(a) and (b) show views from downstream of the shroud vortices for blade B with smoke introduced in shroud boundary layers at the leading edge near the pressure surface. These two vortices are of the type frequently called "passage vortices." Figure 8(a) shows the vortex that forms off the suction surface near the outer shroud, and figure 8(b) the vortex that forms off the suction surface near the hub. This hub passage vortex is of particular interest, because it forms in a region where there is a large accumulation of low-momentum air, including boundary-layer air from both shrouds. The smoke moved from the pressure surface of one blade to the suction surface of the adjacent blade and rolled up on the suction surface. The rotation in this vortex was observed to be clockwise when viewed from downstream.

Figure 8(c) shows the results when smoke was introduced into the suction-surface boundary layer at the leading edge and at approximately blade midheight. As the smoke approached the trailing edge, it turned

toward the hub into the suction-surface radial-flow path and rolled up in a counterclockwise direction. Figure 8(c) indicates that there are two counterclockwise vortices, one above the clockwise vortex shown in figure 8(b) and a very small second one below the clockwise vortex in the extreme corner between blade and hub. Both the counterclockwise vortices appear to contain low-momentum air that results from radial flow from points higher on the blade suction surface as well as cross-channel hub boundary-layer air; whereas, the clockwise vortex appears to contain only the cross-channel hub boundary-layer air. The combination of vortices shown in figures 8(b) and (c) indicates the extent of the hub loss region.

Double boundary layer. - The cross-channel component of hub boundary-layer flow that results in the array of vortices of figures 8(b) and (c) may be an example of a "double" boundary layer. This cross-channel component cannot be represented as a boundary layer having vorticity in a single direction, as can a boundary layer in which the velocity has the mainstream direction (fig. 9(a)), because the cross-channel component of velocity is zero not only at the hub but also where it joins the mainstream. However, a "double" boundary layer with two oppositely directed vorticities can represent the situation (fig. 9(b)). Viewed from downstream, the vorticity in the part of the cross-channel boundary-layer component nearer to the mainstream would be clockwise; that in the sublayer next to the wall would be counterclockwise. When the boundary layer reaches the suction-surface corner, the confluence of low-momentum fluid from cross-channel flow and from radial flow results in the development of these vorticities into concentrated vortices. The general downstream motion of the flow field then makes observation of the vortices possible, as shown in figures 8(b) and (c). The clockwise vortex shown in figure 8(b) is larger than the others, is more easily observed, and is the one generally referred to as a "passage vortex." Reference 3 indicates that sub-boundary-layer thickness for such a typical "double" boundary layer is approximately one-sixth of the total boundary-layer thickness. Loos (ref. 4) also discusses transport of vorticity and thickness of the sublayer for a "double" laminar boundary layer.

Flow-area blockage. - The effect of flow-area blockage resulting from the presence of the loss region near the hub is shown in figure 10. Smoke was introduced at three circumferential positions, at the hub ahead of the nozzle blade row, so that the smoke would indicate free-stream flow as the probe was moved circumferentially. Near the blade pressure surface (fig. 10(a)) the smoke pattern indicated the presence of no appreciable accumulation of low-momentum air. Figure 10(b) shows that, when the smoke was introduced near the suction surface, the pattern moved away from the hub. Finally (fig. 10(c)), the smoke passed over the vortex region in the corner between the hub and suction surface, indicating that the low-momentum air in the hub loss region acts as a constriction in the passage. Disturbance of the mainstream pattern in the

vicinity of this hub loss region was reflected in the nozzle discharge-angle gradients measured at high air velocities in reference 2. Thus, although the fraction of flow area involved is small, there may be appreciable effects on downstream blade row performance due to these changes in flow velocity.

Effect of a Downstream Rotor

The effects on the nozzle secondary-flow pattern produced by motion of a downstream rotor blade row were photographed for each of the two nozzle blade designs at two rotor speeds. The following table gives the resulting rotor blade angle of incidence at mean radius and the ratio of rotor speed to axial airspeed at the mean radius for each of the conditions studied:

Blade	$\frac{\text{Mean rotor speed}}{\text{Mean axial airspeed}}$	Rotor blade angle of incidence at mean radius, deg
A	0.2	+10
	.9	-12
B	0.2	+14
	.9	-3

Speed measurements were rough, and data in the table are presented as order-of-magnitude values.

A change in the circumferential position of a downstream rotor blade with respect to a nozzle blade means a change in the position of the pressure pattern across the rotor passage inlet relative to the nozzle trailing edge. At low airspeeds, the effect of this pressure-pattern movement might reasonably be expected to extend upstream as far as the nozzle trailing edges with appreciable amplitude. The resulting effect on nozzle secondary-flow paths (wakes and thickened boundary layers) may vary from an increase in local pressure and increased flow-path thickness to a decrease in local pressure and reduced flow-path thickness. One rotor position might, then, be expected to result in an increase in radial flow and another in a decrease in radial flow.

For nozzle blade A, figures 11(a) and (b) show radial flows greater and less, respectively, than that for the isolated nozzle cascade, caused by two different positions of an adjacent stationary rotor blade. Figure 12 shows this effect on nozzle blade B, for which there appears in no case a radial flow greater than that which occurs with the isolated nozzle cascade.

A rotor moving so that the speed ratio was 0.2 caused a pulsation of the nozzle radial flow. For this speed ratio and blade setting, the

rotor blade incidence angle was +10° for blade A and +14° for blade B. Other blade settings might result in rotor passage inlet pressure distributions sufficiently different to cause different magnitudes of rotor effect on nozzle radial flow.

At a speed ratio of 0.9, the nozzle radial flow appeared to be limited by the short duration of the portion of the pressure disturbance for which noticable radial-flow paths existed. That is, periodically, before the slow-moving radial-flow air had traversed an appreciable distance, the radial-flow-path cross-sectional area may have been constricted by the pressure change. It should be remembered that the effect observed photographically is only that pertaining to low-momentum air originating near the outer shroud, since the smoke entry was at that point and therefore traced out only that part of flow. However, it appears that, for blade boundary-layer air entering the radial-flow paths at any other radius, the relatively rapid rotor movement would tend to limit the radial distance of travel of such air before it is swept downstream in the nozzle wake.

At the airspeeds used in turbine operation, it cannot be assumed that rotor effects on nozzle radial flow would have the magnitudes shown for the low airspeed of this investigation. For subsonic axial airspeeds, the approach of a pressure peak located near the rotor leading edge toward a given nozzle would be felt at the nozzle as a pressure increase, the amplitude of which might be expected to depend upon the following factors:

(1) Amplitude of the disturbance at its origin, which might be greater for higher airspeeds

(2) Rate of reduction in amplitude with distance traveled upstream from the rotor, which might in turn depend on the airspeed

(3) Turbulence in the air through which the disturbance travels, which would tend to smooth out pressure peaks

In an actual turbine, therefore, such pressure variations may affect nozzle secondary flows, or may exist with amplitudes too small to affect nozzle secondary flows appreciably or to be detected by a pressure-sensitive probe.

SUMMARY OF RESULTS

The following results were obtained from a visual and photographic study of the smoke patterns of secondary flow in two cascades of turbine nozzles. Both still and motion pictures were used, and airspeed was kept low.

1. The smoke showed secondary-flow patterns similar to those indicated by kinetic-energy loss distributions based on pressure and flow-angle measurements of these two nozzle configurations at high airspeeds.

2. Secondary-flow patterns visualized by smoke agree with loss distributions from previous pressure and angle measurements in indicating that blade shape and suction-surface velocity profile have considerable effect on the secondary-flow pattern in turbine nozzles. Smoke patterns indicated that, for the poorer profile blade, the greater portion of inward radial transport of low-momentum fluid took place along the suction surface near the trailing edge and reached the hub. For the other blade profile, however, the inward radial transport of low-momentum air took place mainly in the wake at the trailing edge of the blade, and a large portion of the low-momentum air was swept downstream in the blade wake during radial transport.

3269

2-ED

3. A low-speed rotating blade row downstream of an annular cascade of nozzle blades produced a periodic disturbance of radial secondary flows which exist in the nozzle trailing-edge region. The effect may be due to pressure fluctuations associated with the moving rotor. For the airspeed used, an increase in rotor speed resulted in an increased frequency of disturbance that prevented the outer-shroud boundary-layer air entering the radial-flow region from moving an appreciable distance toward the hub. It is expected that air entering the radial-flow path from the suction-surface boundary layer would be affected in the same way. This effect may exist in some form also at actual turbine operating conditions.

Lewis Flight Propulsion Laboratory
National Advisory Committee for Aeronautics
Cleveland, Ohio, August 2, 1954

REFERENCES

1. Herzig, Howard Z., Hansen, Arthur G., and Costello, George R.: A Visualization Study of Secondary Flows in Cascades. NACA Rep. 1163, 1954. (Supersedes NACA TN 2947.)

2. Rohlik, Harold E., Kofskey, Milton G., Allen, Hubert W., and Herzig, Howard Z.: Secondary Flows and Boundary-Layer Accumulations in Turbine Nozzles. NACA Rep. 1168, 1954. (Supersedes NACA TN's 2871, 2909, and 2989.)

3. Mager, Artur, and Hansen, Arthur G.: Laminar Boundary Layer over Flat Plate in a Flow Having Circular Streamlines. NACA TN 2658, 1952.

4. Loos, Henk G.: Analysis of Secondary Flow in the Stator of an Axial Turbomachine. Tech. Rep. No. 3 to Office Sci. Res., Air Res. and Dev. Command, GALCIT, Sept. 1953.

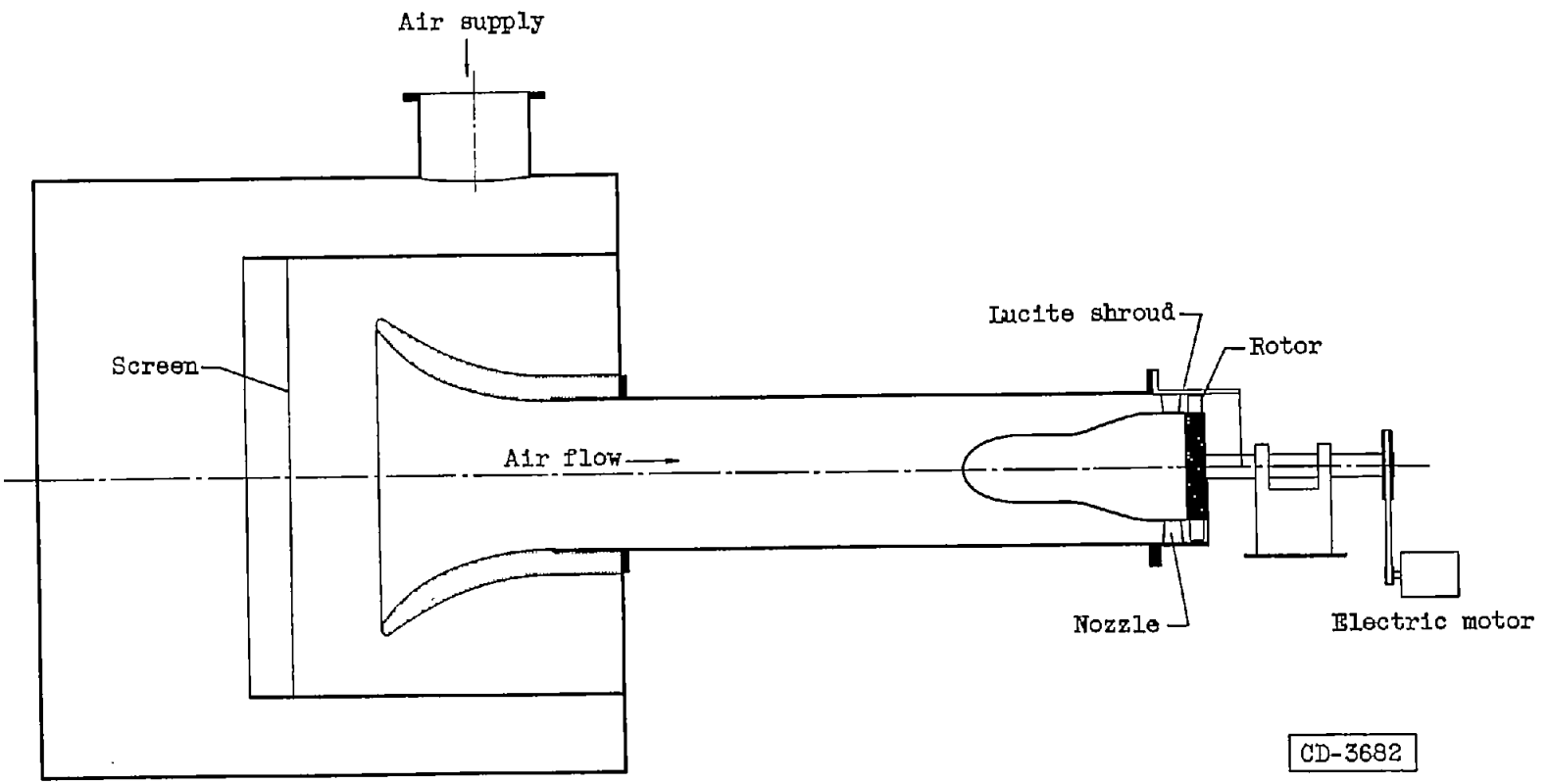

Figure 1. - Schematic view of annular cascade.

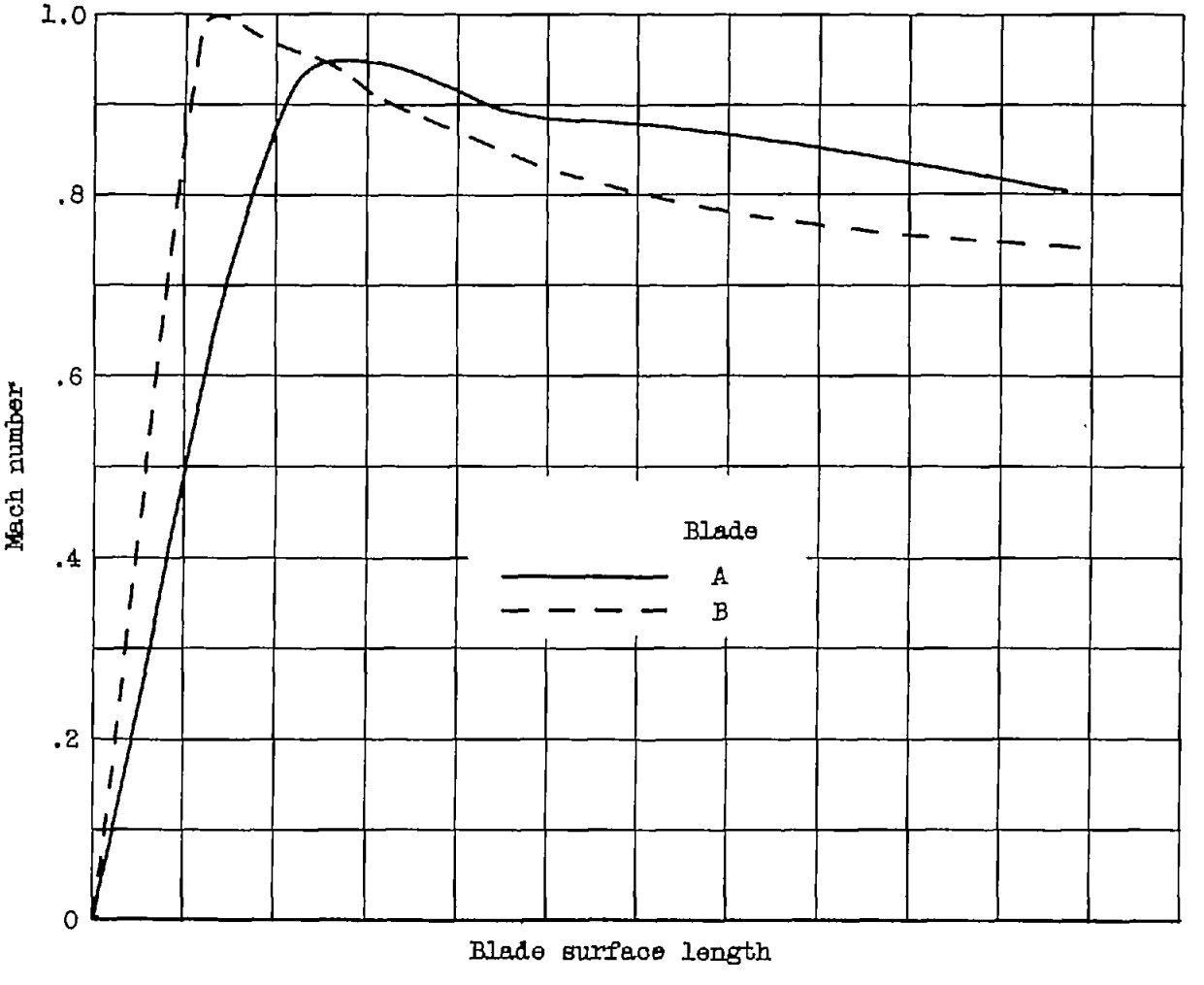

(a) Hub section.

Figure 2. - Design velocities for blade suction surface.

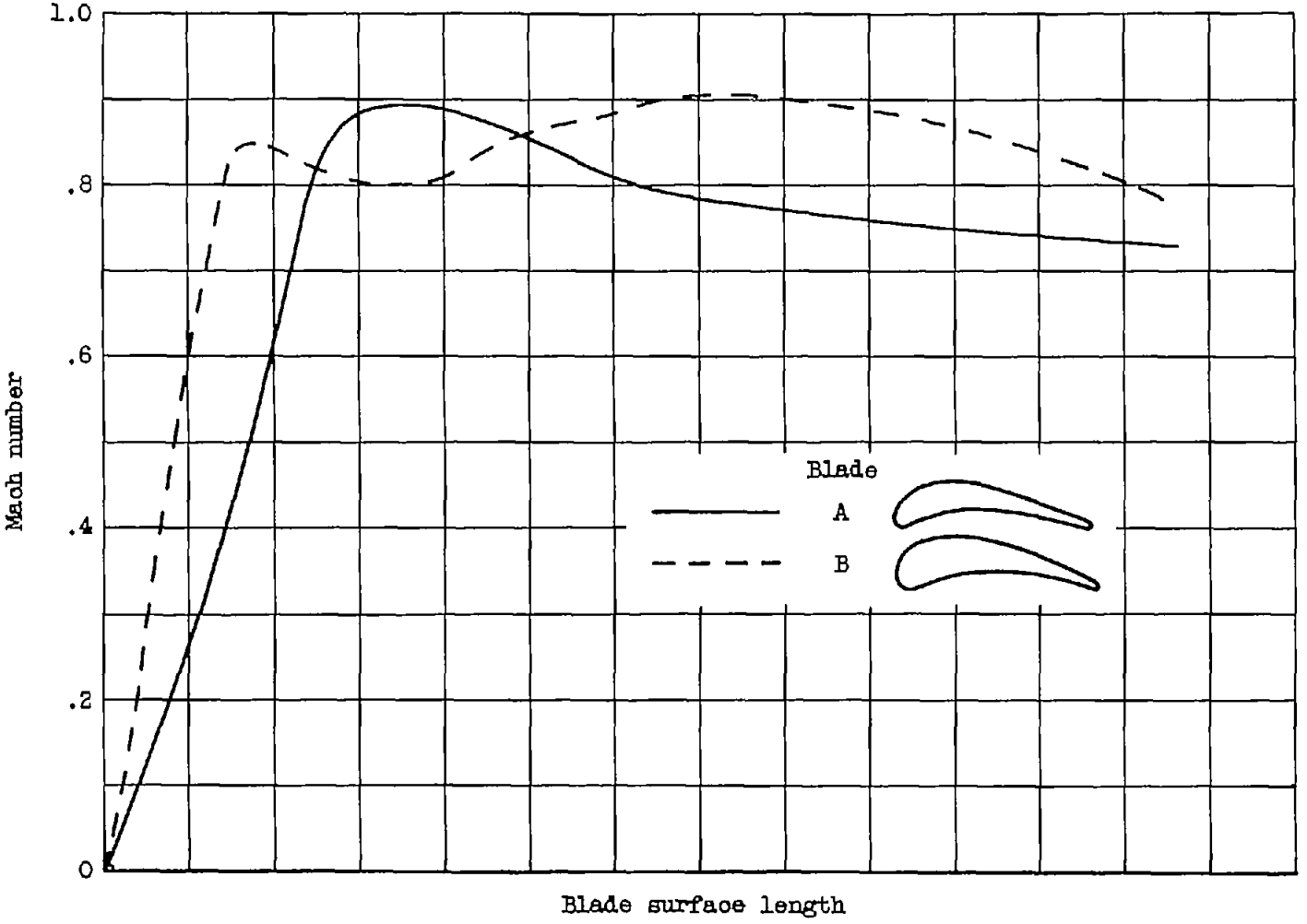

(b) Mean section.

Figure 2. - Continued. Design velocities for blade suction surface.

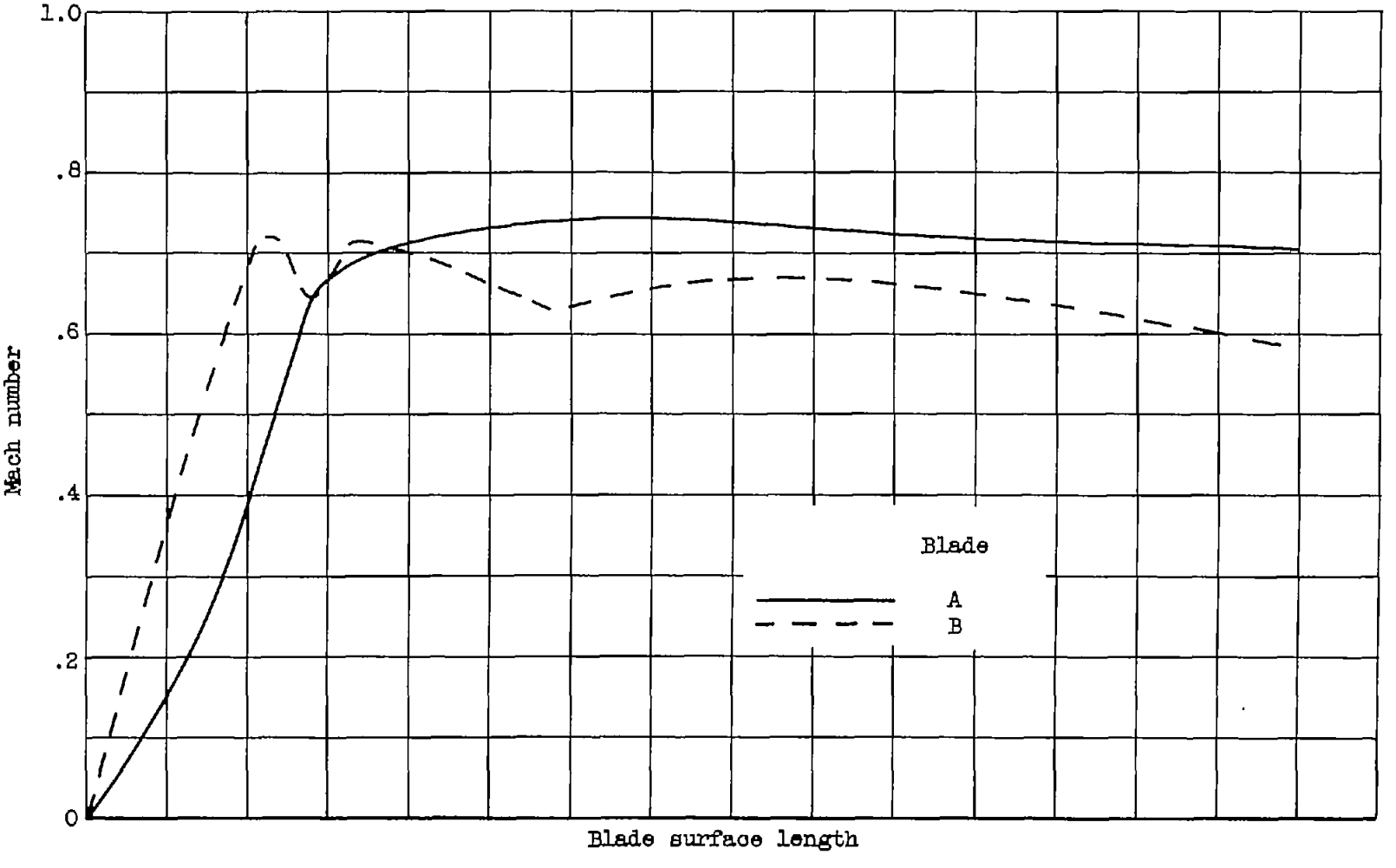

(c) Tip section.

Figure 2. - Concluded. Design velocities for blade suction surface.

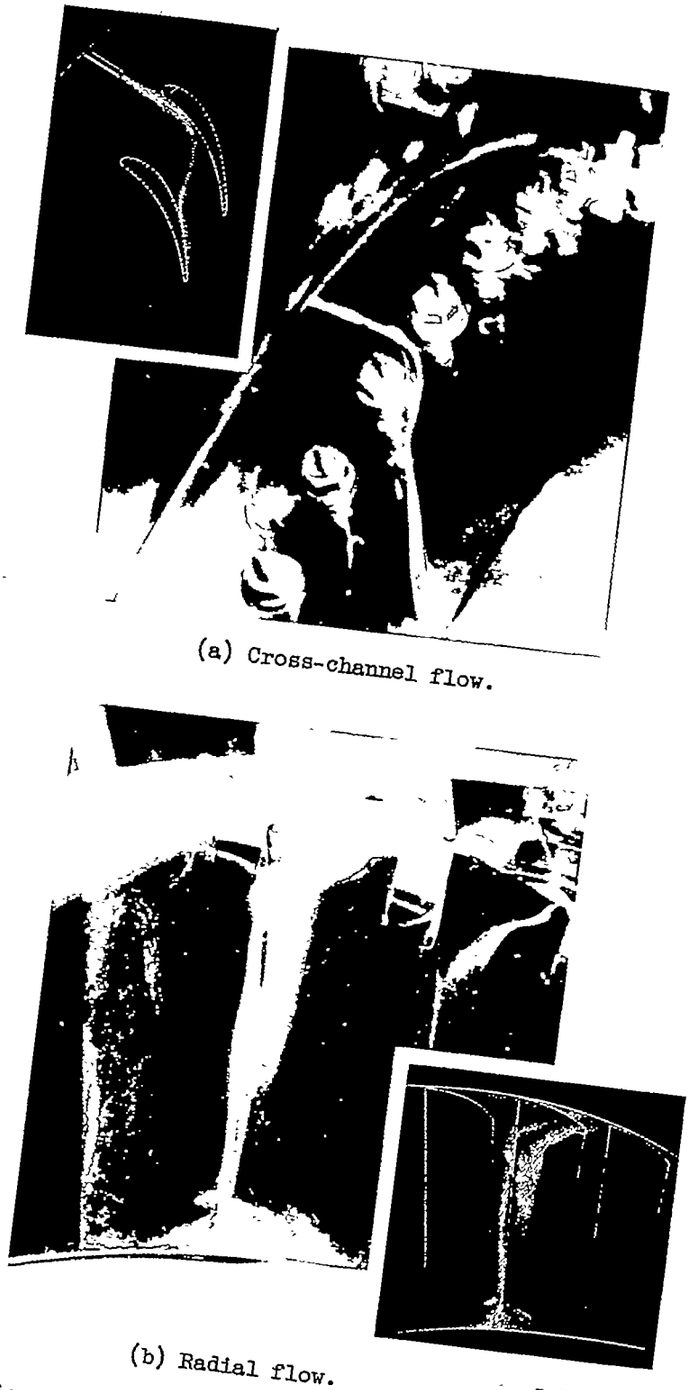

(a) Cross-channel flow.

(b) Radial flow.

C-36416

Figure 3. - Secondary flows for blade B.

(a) Smoke entering passage continuously.

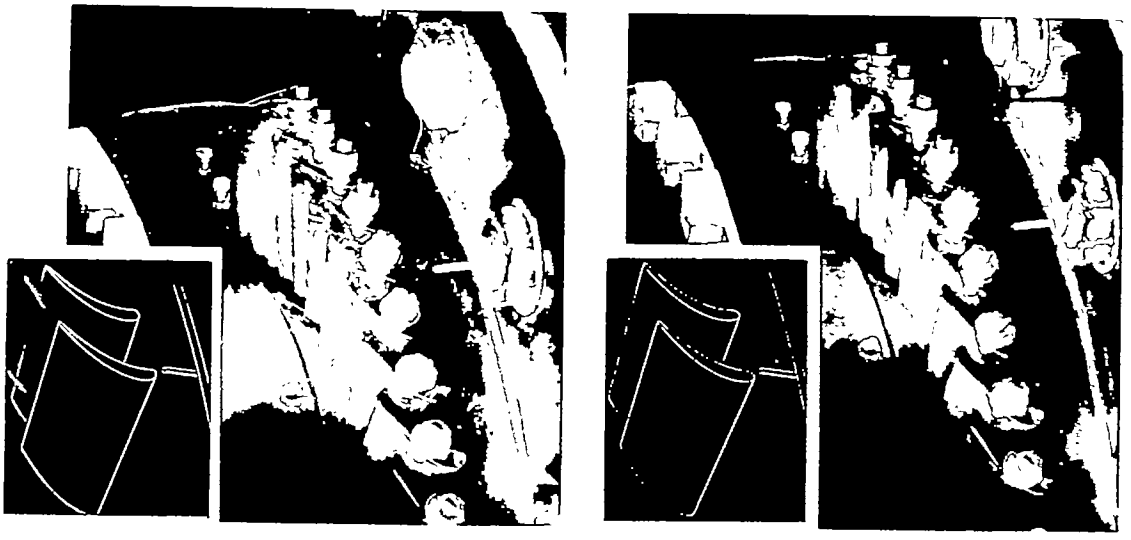

C-36417

(b) About 0.15 second after smoke is cut off. Inner and outer shroud cores visible.

(c) About 0.45 second after smoke is cut off. No visible trace of smoke remaining.

Figure 4. - Retention of smoke in loss regions for blade B.

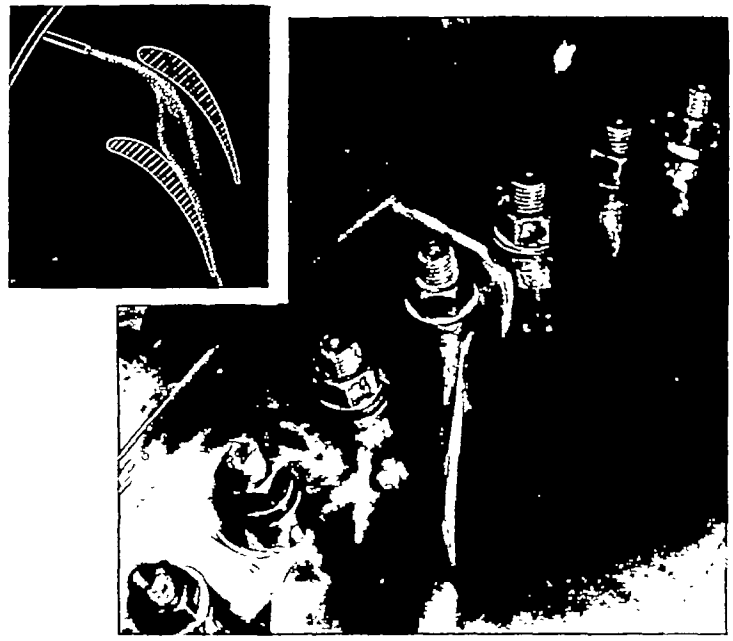

(a) Cross-channel flow.

C-36418

(b) Radial flow.

Figure 5. - Secondary flows for blade A.

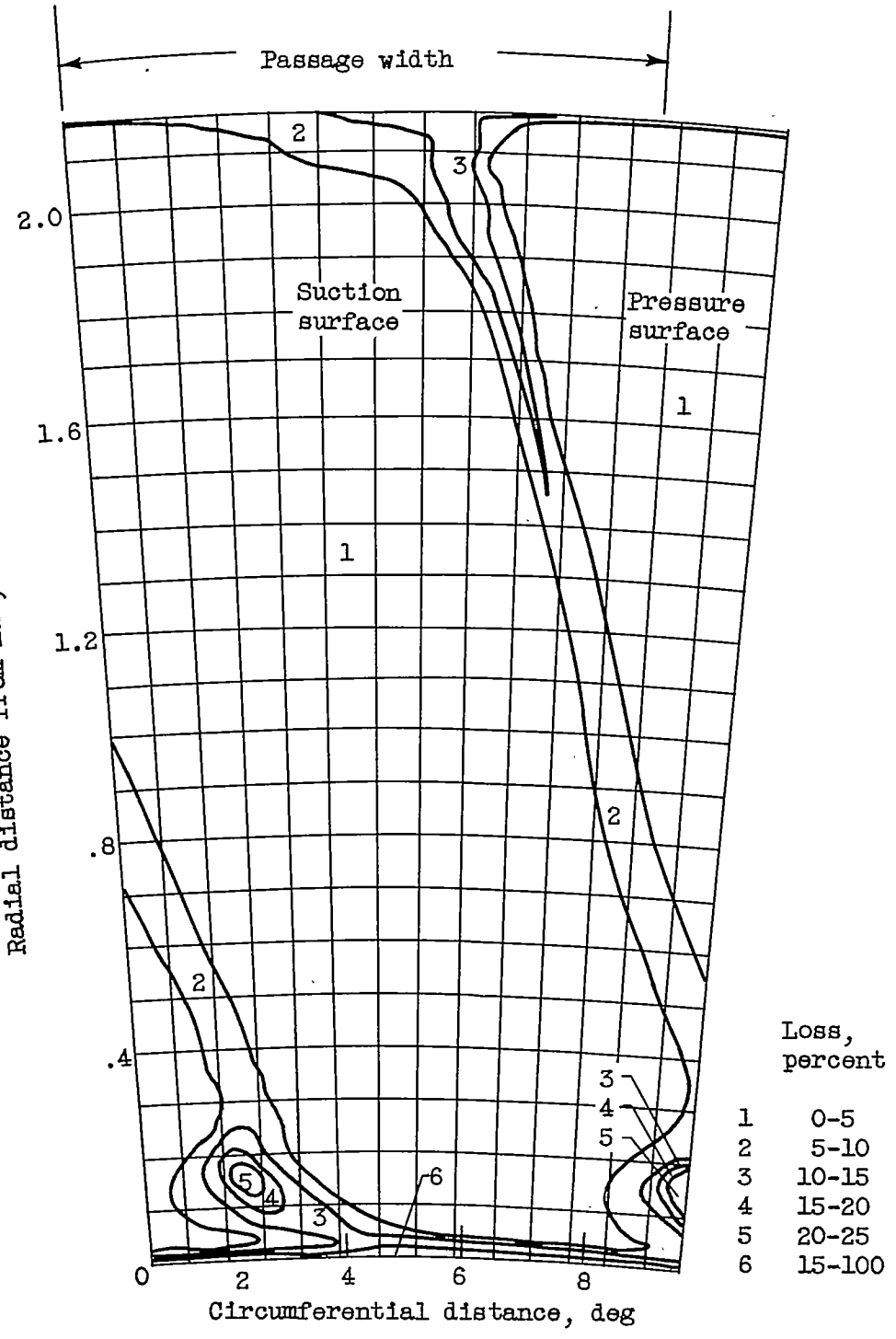

(a) Blade A; hub Mach number, 0.86.

Figure 6. - Contours of loss across one blade passage.

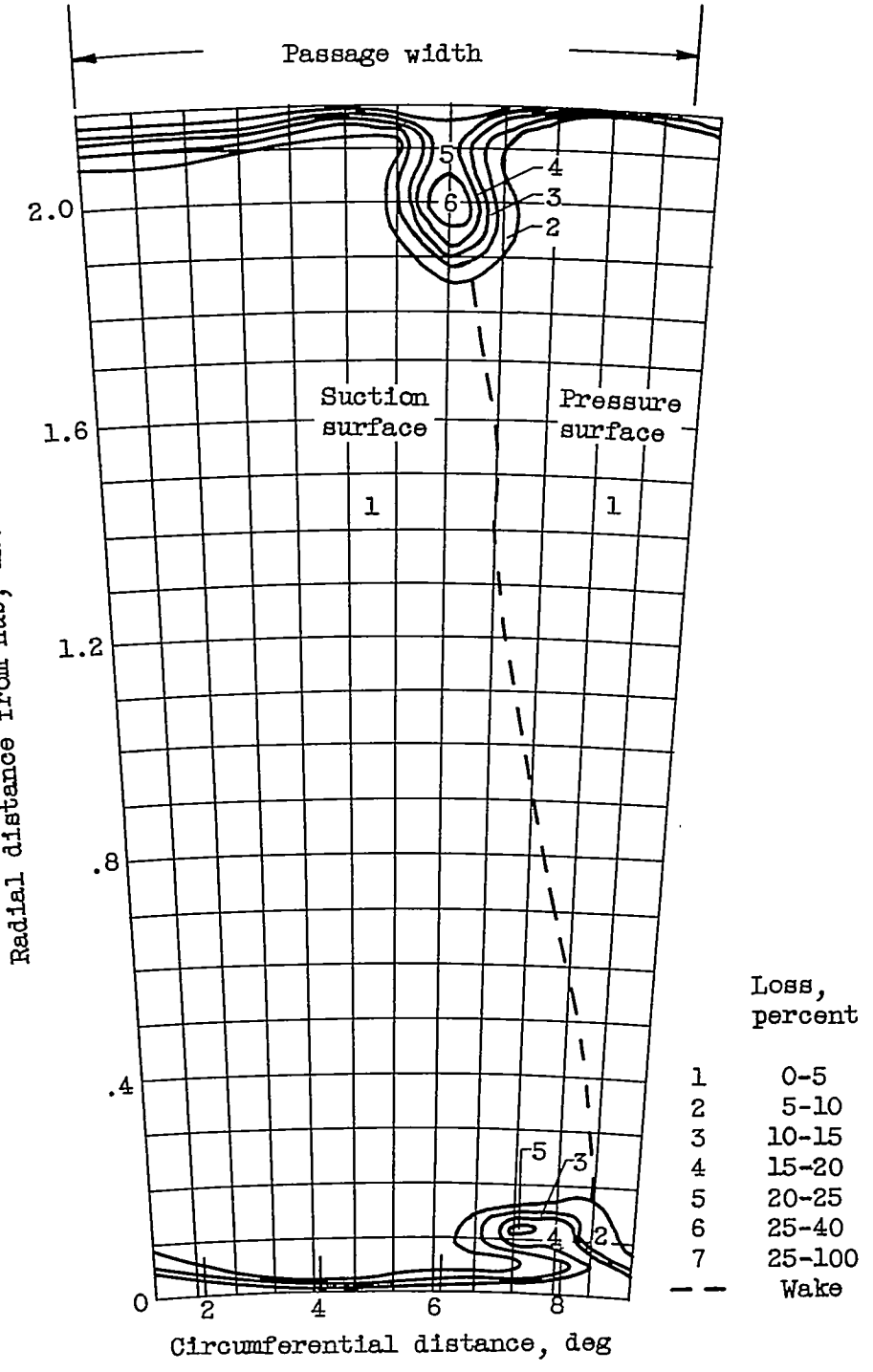

(b) Blade B; hub Mach number, 1.18.

Figure 6. - Concluded. Contours of loss across one blade passage.

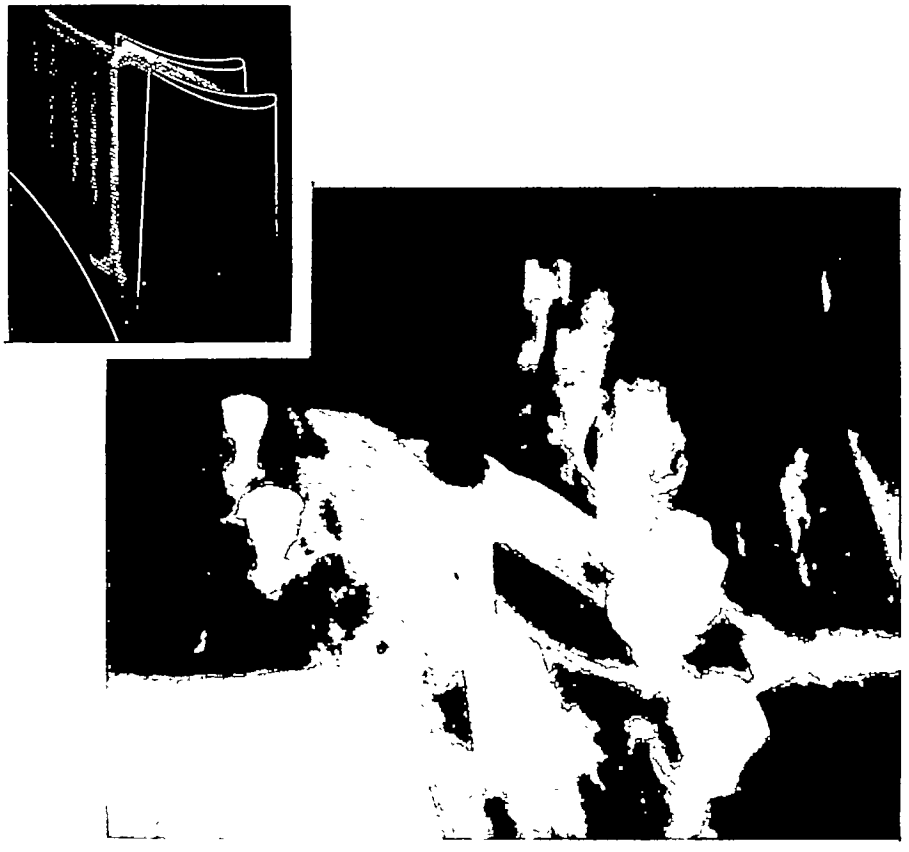

C-36419

Figure 7. - Columnar wake flow for blade A.

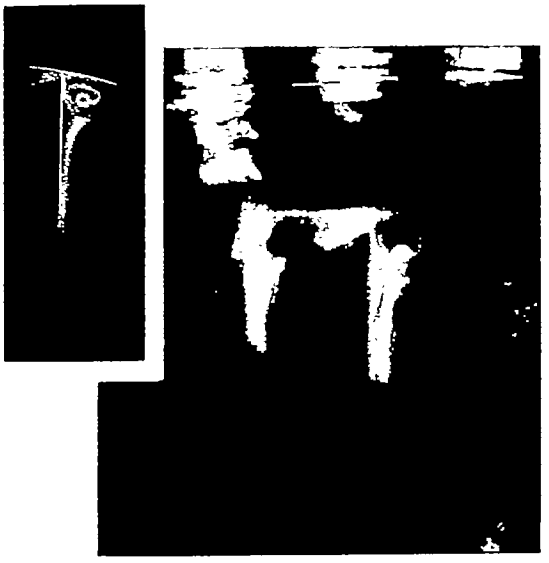

(a) Outer-shroud vortex from downstream for blade B.

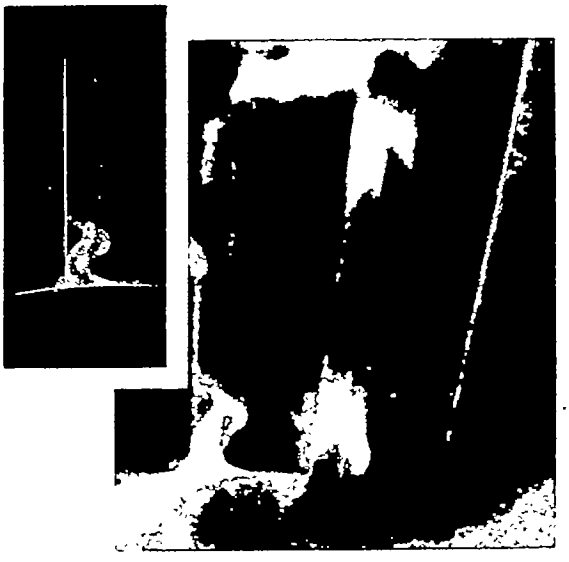

(b) Clockwise roll-up on suction surface at hub for blade B.

C-36420

(c) Counterclockwise vortices at hub for blade B.

Figure 8. - Blade B loss regions.

3269

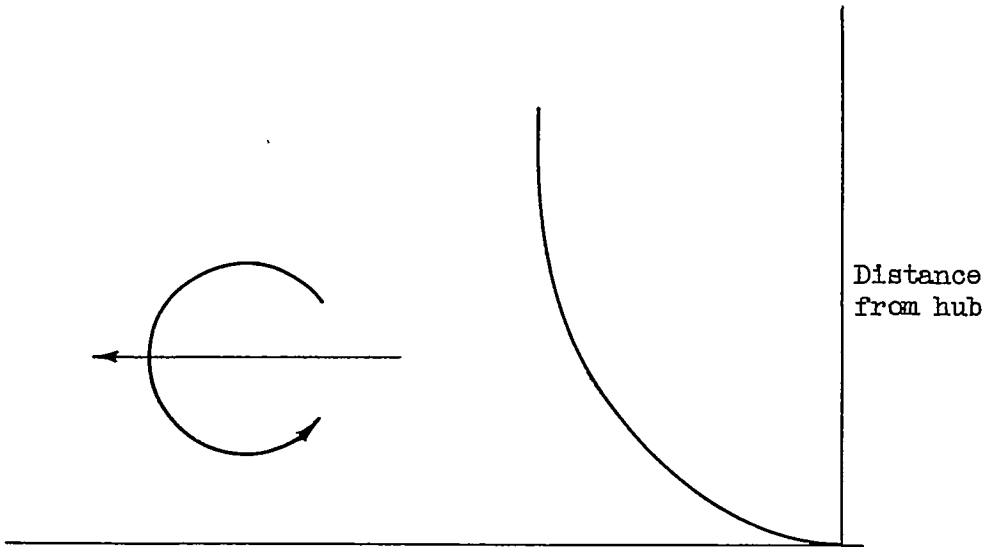

(a) Component of boundary layer in mainstream direction.

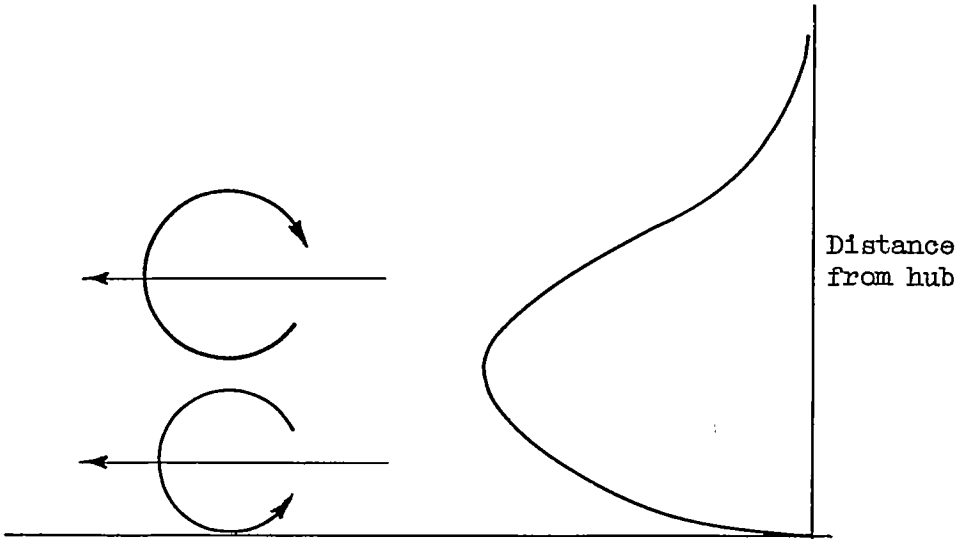

(b) Cross-channel component of boundary layer.

Figure 9. - Boundary-layer vorticities and velocity profiles.

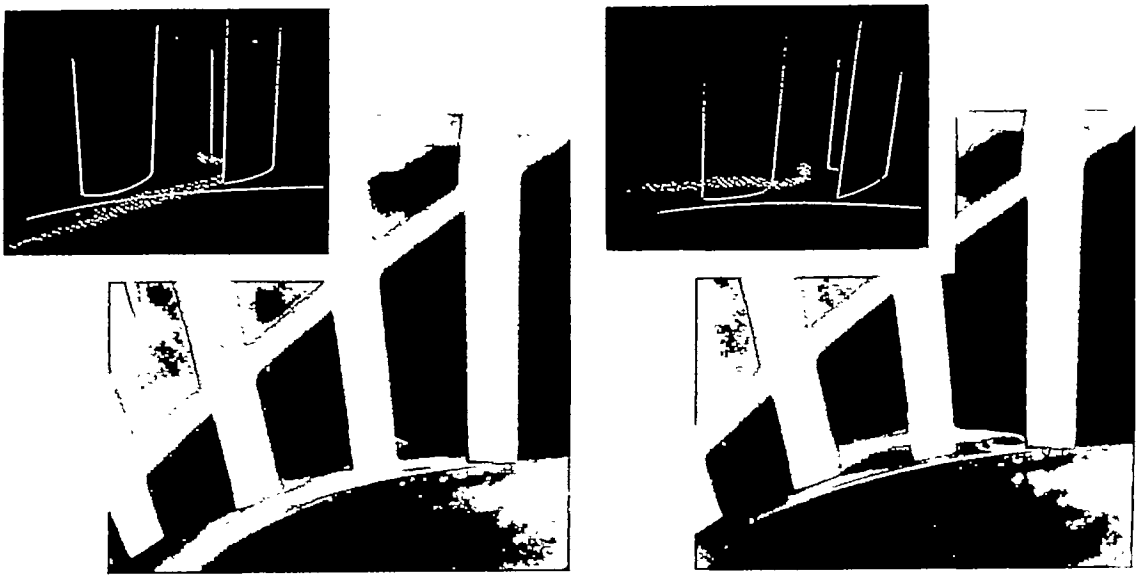

(a) Streamlines near pressure surface.

(b) Streamlines in midpassage.

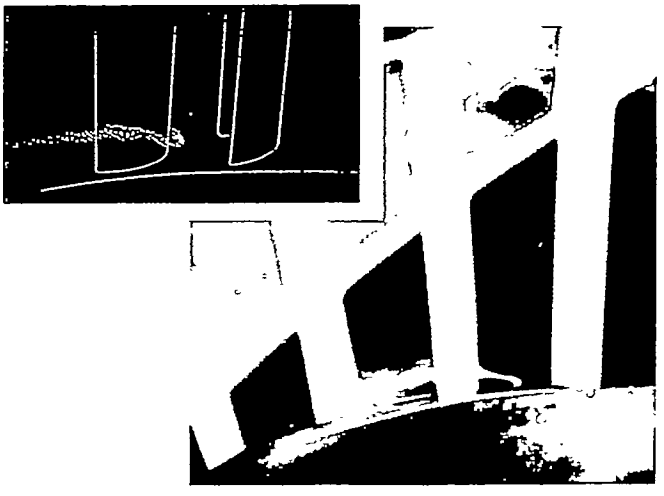

C-36421

(c) Streamlines near suction surface.

Figure 10. - Deviation of main flow streamlines due to accumulation of low-momentum air.

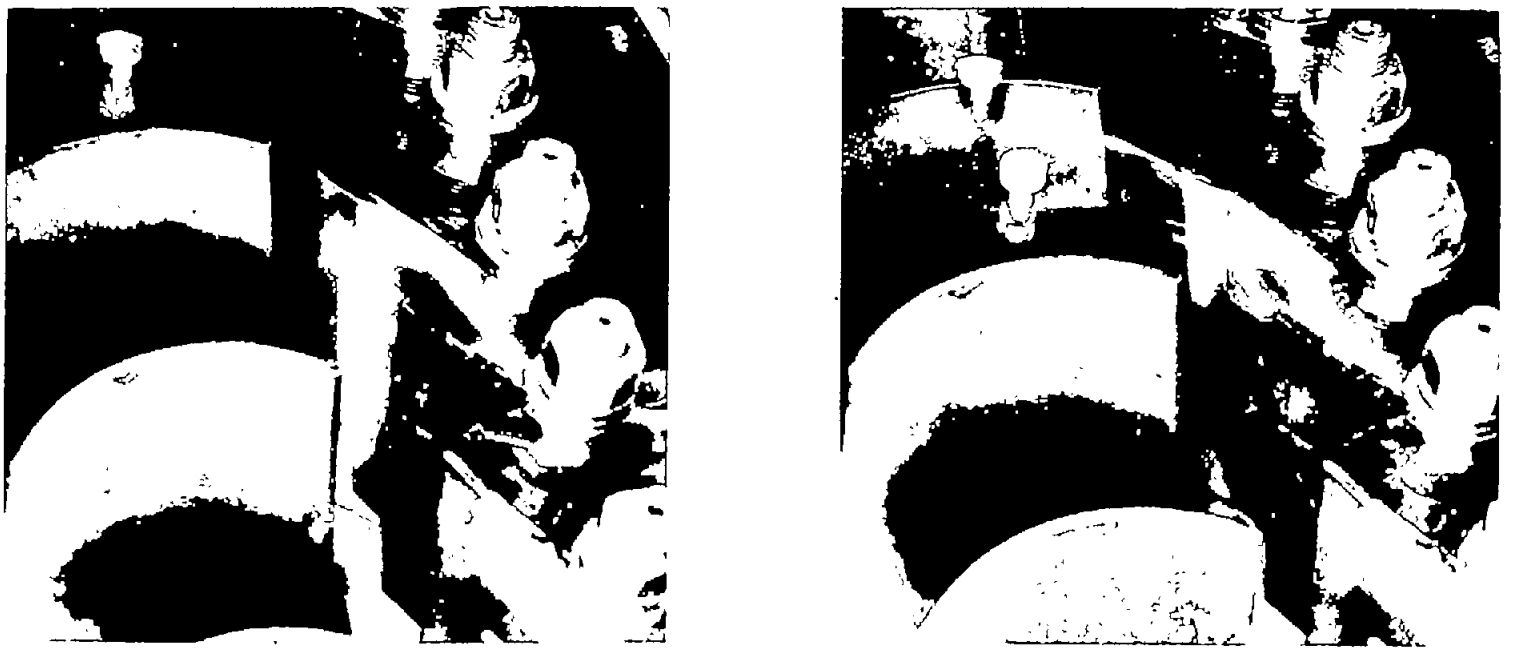

(a) First rotor position.

(b) Second rotor position.

C-36422

Figure 11. - Effect of rotor blade position on radial flow for nozzle blade A.

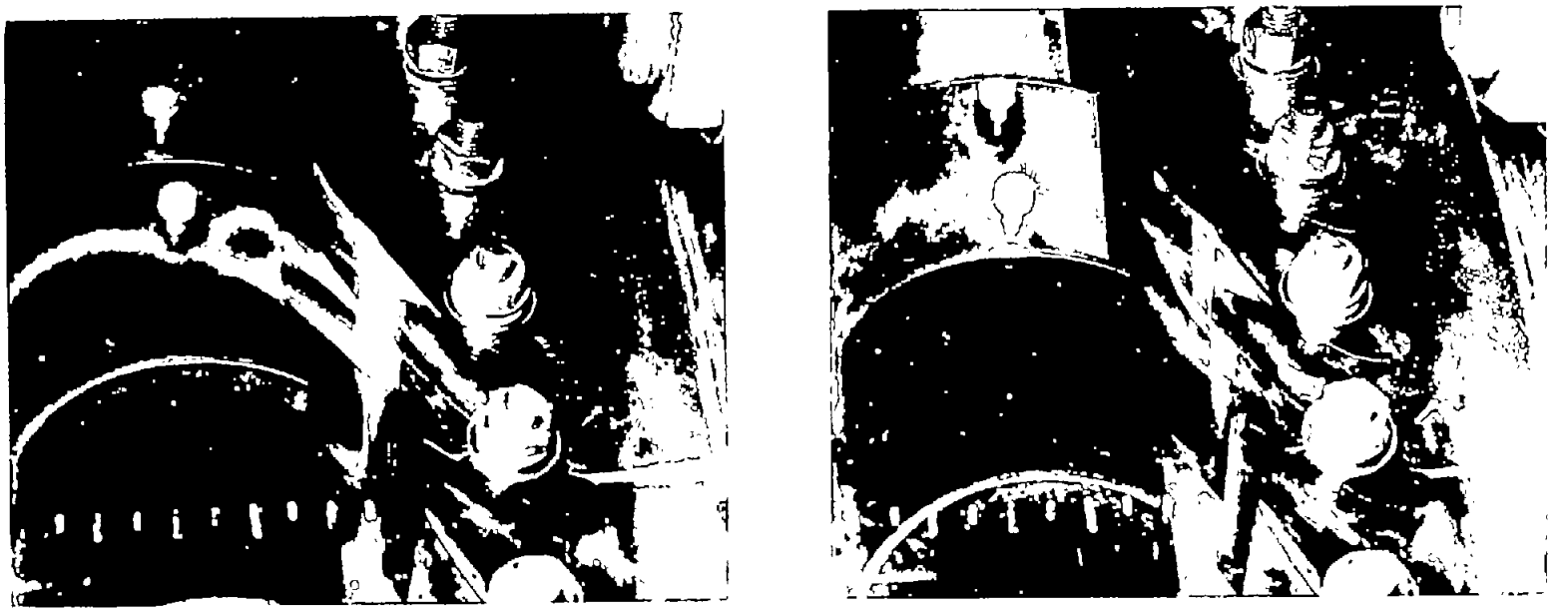

C-36423

(a) First rotor position.

(b) Second rotor position.

Figure 12. - Effect of rotor blade position on radial flow for nozzle blade B.

NACA-Langley - 11-2-54 - 1000